Int. J. Electrochem. Sci., 15 **(2020)** 7298 – 7309, doi: 10.20964/2020.08.53

International Journal of
ELECTROCHEMICAL
SCIENCE
www.electrochemsci.org

Amino-functionalized MIL Type Metal Organic Frameworks as Heterogeneous Catalysts for Asymmetric Electrocarboxylation of (1-chloroethyl)benzene with CO_2

Hui Wang, Zhuo-Lin Wang, Yi-Jun Zhao, Yi Shi, Huan Wang and Jia-Xing Lu**

Shanghai Key Laboratory of Green Chemistry and Chemical Processes, School of Chemistry and Molecular Engineering, East China Normal University, Shanghai 200062, P. R. China.
*E-mail: hwang@chem.ecnu.edu.cn; jxlu@chem.ecnu.edu.cn

Received: 5 March 2020 / *Accepted:* 11 May 2020 / *Published:* 10 July 2020

Due to the high specific surface area and tunable pore size of Metal-Organic Frameworks (MOFs), the use of MOFs to catalyze CO_2 conversion has increased in recent years. The present study is the first to use three MOFs of MIL types with free amino groups, namely, MIL-101-NH_2(Cr), MIL-101-NH_2(Al) and MIL-53-NH_2(Al), for asymmetric electrocarboxylation of (1-chloroethyl)benzene with CO_2. The electrochemical behavior of three MOFs were discussed. The optically active 2-phenylpropionic acid was obtained using t-Bu(R,R)salen(Co[II]) as the chiral mediate under mild conditions. In order to get the optimal results, the reaction conditions such as the influence of temperature, charge and the quantity of catalysts were investigated.

Keywords: MOFs; CO_2; Asymmetry; Electrocarboxylation; (1-chloroethyl)benzene

1. INTRODUCTION

The dramatic increase of CO_2 in the atmosphere is among the world's biggest environmental problems [1]. CO_2 is the most important and abundant carbon resource in nature. CO_2 as the reactant in chemical reaction can be cleanly and efficiently converted into other chemicals [2, 3]. Fixing CO_2 via electroorganic synthesis is a novel green synthetic method because of its mild conditions and simple process [4-6]. Electrocarboxylation of organic compounds in the CO_2 environment to produce the corresponding carboxylic acid is one of the effective methods for fixing CO_2 [7, 8]. Optically active carboxylic acids have important applications in medical, agricultural, and fine-chemical production. However, few reports [9, 10] on asymmetric electrocarboxylation have been published due to difficulty in stereoselective immobilization of CO_2. In our previous work [11], optically active 2-phenylpropionic acid, which has excellent pharmacological activity, was successfully synthesised from asymmetric

carboxylation of (1-chloroethyl)benzene with the help of electroreduced chiral $[Co^{I}(salen)]^-$ complex. It can bind to the substrate during the reaction process to help the formation of chirality.

Generally, metal plate electrodes are the most widely used electrodes in electrochemistry, especially in electroorganic synthesis systems [12, 13]. However, electrocatalytic reaction sites for the substrates are limited due to the limitation of the geometric areas of plate electrodes. MOFs are a class of hybrid materials composed of metal ions or clusters coordinated by organic ligands. MOFs has a high specific surface area, an adjustable structure and good thermal stability. Thus, MOFs have potential applications in many fields, such as gas storage, molecular separations, heterogeneous catalysis and drug delivery [14-18]. Currently, an increasing number of reports about MOFs use in electrocatalysis is available [19, 20]. Moreover, MOFs can be applied in asymmetric catalysis [21, 22]. Compared with other MOFs, MIL types have relatively high thermal and chemical stability, excellent porosity and high specific surface area; thus these materials can be used to catalyse macromolecular reactions [23, 24]. Meanwhile, MOFs are superior to zeolite, silica, and metal oxides in terms of CO_2 adsorption [25-28] due to not only the good porosity and specific surface area of MOFs, but also the free groups on MOFs which can interact with CO_2. MOFs functionalized with NH_2 group, could be potential catalyst candidates for the CO_2 conversion [29-31]. Therefore, amino-modified MOFs can be used as catalysts for CO_2 adsorption and conversion and as heterogeneous catalysts for CO_2 conversion.

In the present paper, three amino-functionalized MIL types of MOFs, namely, MIL-101-NH_2(Cr), MIL-101-NH_2(Al) and MIL-53-NH_2(Al), were prepared and used for asymmetric electrocarboxylation of (1-chloroethyl)benzene [$PhCH(CH_3)Cl$]. Various characterisations have been performed to check the morphology and composition of these materials. In addition, the cyclic voltammetric behaviour of these materials were explored. The optically active 2-phenylpropionic acid can be achieved with chiral t-Bu(R,R)salen(Co[II]) as chiral mediate via potentiostatic electrolysis under mild conditions.

2. EXPERIMENTAL

2.1. Materials

2-nitroterephthalic acid and 2-aminoterephthalic acid were purchased from Innochem Chemical. $AlCl_3 \cdot 6H_2O$, $Cr(NO_3)_3 \cdot 9H_2O$, $SnCl_2 \cdot 2H_2O$, N,N-dimethylformamide (DMF), tetraethylammonium iodide (TEAI), hydrochloric acid (HCl, 36.0%~38.0%), methyl alcohol, ether, anhydrous magnesium sulfate were purchased from Sinopharm Chemical. $PhCH(CH_3)Cl$ was purchased from TCI. t-Bu(R,R)salen(Co[II]) was purchased from J&K Chemical.

2.2. Synthesis of MIL-101-NH_2(Cr)

MIL-101-NH_2(Cr) was synthesised using a literature method [31] by means of a solvothermal treatment involving 10 mL distilled water as solvent. Starting reactants were arechromium(III)nitrate nonahydrate ($Cr(NO_3)_3 \cdot 9H_2O$, 99%, 0.815 g), 2-nitroterephthalic acid (99.5%, 0.445 g) and hydrofluoric

acid (HF, 40%, 87 μL). The reactants were placed in a Teflon vessel and stirred for 20 min and then inserted into a stainless steel autoclave, heated up to 493 K and kept for 8 h. The resulting green product MIL-101-NO_2(Cr), was filtered out and washed with boiling methanol for 12 h, and finally dried in air overnight at 353 K. 100 mg of MIL-101-NO_2(Cr), 3.26 g of $SnCl_2 \cdot 2H_2O$ and 20 mL of methanol were mixed and reacted at 343 K for 12 h. The obtained solid was centrifuged, and then stirred for 30 min in 20 mL concentrated hydrochloric acid and washed with H_2O until pH = 7. At last, the obtained green solid, MIL-101-NH_2(Cr), was dried in air at 373 K for 12 h.

2.3. Synthesis of MIL-53-NH_2(Al)

MIL-53-NH_2(Al) was synthesised by hydrothermal method according to procedures described in literature [32]. Briefly, 0.724 g (3.0 mmol) of $AlCl_3 \cdot 6H_2O$ and 0.543 g (3.0 mmol) of 2-aminoterephthalic acid were dissolved in 15 mL of distilled water, respectively. The dissolved $AlCl_3 \cdot 6H_2O$ was added dropwise to 2-aminoterephthalic acid solution and stirred for 1 h. The resulting solution was placed in a hydrothermal reactor and reacted at 423 K for 5 h. The obtained solid was washed successively with water and DMF, and then washed in 20 mL of DMF at 353K for 24 h and then immersed in methanol for 72 h. Lastly, MIL-53-NH_2(Al) was dried under vacuum at 343 K for 24 h.

2.4. Synthesis of MIL-101-NH_2(Al)

The synthesis method of MIL-101-NH_2(Al) was as follows as the literature [33]: 272 mg (1.5 mmol) of 2-aminoterephthalic acid was dissolved in 60 mL of DMF and heated to 383 K in an oil bath. 724 mg (3 mmol) of $AlCl_3 \cdot 6H_2O$ was divided into seven equal portions, and each was added to the previous DMF solution every 15 min. The solution was stirred at 383 K for 3 h and without stirring for 16 h. After the reaction, the mixture was cooled to room temperature. The obtained yellow solid was washed with DMF and ethanol, and then refluxed with ethanol for 24 h. After drying, MIL-101-NH_2(Al) was obtained.

2.5. Characterization

X-ray diffraction (XRD) patterns were recorded by a Ultima IV X-ray diffractometer using Cu Kα radiation (k= 1.5406 Å) at a scanning rate 10 °/min. Fourier transform infrared (FT-IR) spectra were recorded by a Nexus 870 FT-IR spectrometer. Nitrogen adsorption-desorption and carbon dioxide adsorption isotherm measurements were carried out on a Micromeritics, ASAP2020. Yields and enantiomeric excess (ee) were detected by high-performance liquid chromatography (HPLC) (DIONEX U-3000 pump) equipped with a UV detector and a chiralcel AD-H column (DAICEL Chiral technologies CO., Ltd.). Cyclic voltammograms (CVs) were recorded on a CHI 600c electrochemical station (Shanghai Chenhua Instruments Company) at 293 K in an undivided cell. MIL-53-NH_2(Al), MIL-101-NH_2(Al) and MIL-101-NH_2(Cr) were coated onto the surface of a glassy carbon electrode (d=2 mm) as

working electrodes respectively. The counter electrode was a Pt net (1.5 cm×1.5 cm). An electrode of Ag/AgI/0.1 M TEAI in DMF was used as the reference electrode.

2.6. Potentiostatic electrolysis

Potentiostatic electrolysis was carried out in an undivided cell. 7.5 mM of t-Bu(R,R)salen(Co[II]), 0.1 M of TEAI and 0.05 M of $PhCH(CH_3)Cl$ were mixed into 10 mL of CO_2-saturated DMF. MIL-53-NH_2(Al), MIL-101-NH_2(Al) and MIL-101-NH_2(Cr) were coated on carbon paper (1.5 cm×1.5 cm) as working electrodes respectively. The counter electrode and reference electrode were Pt net (1.5 cm×1.5 cm) and Ag/AgI/0.1 M TEAI in DMF, respectively (Scheme 1). At the end of the electrolysis, the electrolyte was distilled off the solvent and extracted with diethyl ether. Then the residue was dried with anhydrous magnesium sulfate and the product yield and ee were detected by HPLC.

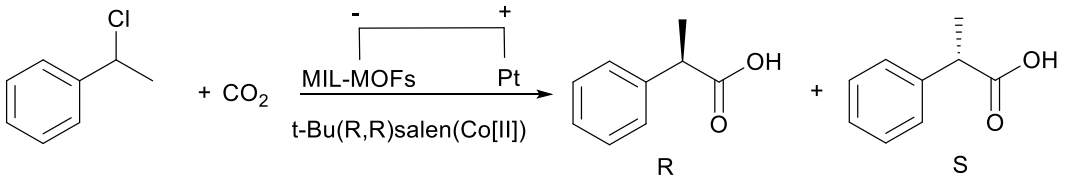

Scheme 1. Asymmetric carboxylation of $PhCH(CH_3)Cl$ with CO_2

3. RESULTS AND DISCUSSION

XRD patterns of the prepared MIL-101-NH_2(Cr), MIL-101-NH_2(Al) and MIL-53-NH_2(Al) are shown in Fig. 1, together with the simulated XRD patterns for MIL-101and MIL-53. The comparison between the experimental and simulated XRD patterns demonstrated MIL-53-NH_2(Al), MIL-101-NH_2(Al) and MIL-101-NH_2(Cr) were synthesized with pure phases, similar to the reports [31-33]. The amino group modification of these three MOFs can be characterised through FT-IR (Fig. 2). The asymmetric and symmetric N–H stretching vibrations of the amino groups were observed at 3465 and 3361 cm^{-1}, respectively. Additionally, the stretching vibration of C–N bond appeared at 1165 cm^{-1}, which are in accordance with previously reported values [31]. This indicated that amino groups existed in the three MIL series MOFs. The N_2 adsorption-desorption curves were measured at 77 K (Fig. 3A), and the parameters of MIL-53-NH_2(Al), MIL-101-NH_2(Al) and MIL-101-NH_2(Cr) were summarized in Table 1. By comparison, MIL-101-NH_2(Cr) had the largest specific surface area, total pore volume and pore size. It showed that MIL-101-NH_2(Cr) has relatively good pore structure. The specific surface area, total pore volume and pore size of MIL-101-NH_2(Al) were not as large as MIL-101-NH_2(Cr), while MIL-53-NH_2(Al) has the smallest parameters of pore. The specific surface area of these three MOFs were similar to literatures [31, 34-36]. CO_2 adsorption measurement and CO_2 adsorption capacity data of these three MOFs were tested at 298 K (Fig. 3B and Table 1), and results showed that MIL-101-NH_2(Cr) had the

largest CO_2 adsorption capacity with the data of 45.28 cm^3 g^{-1}. By contrast, the CO_2 adsorption of MIL-53-NH_2(Al) was relatively small, probably because the adsorption capacity of CO_2 is related to the specific surface area and pore size of the material [25-27]. Among the three materials, MIL-53-NH_2(Al) had the smallest specific surface area and pore size. Hence, its adsorption capacity of CO_2 was relatively low. In addition, the CO_2 adsorption capacity of the material had a great relationship with the amino groups modified on the MOFs [30, 37]. Taken MIL-101-NH_2(Cr) as an example, when the modified group was -NH_2, the adsorption capacity for MIL-101-NH_2(Cr) was 45.28 cm^3 g^{-1}, whereas the data was only 36.70 cm^3 g^{-1} for MIL-101-NO_2(Cr). It was found that amino-functionalized MOFs have a stronger ability to adsorb CO_2 than unfunctionalized MOFs, indicating that the introduction of amino groups is beneficial to improve the ability of MOFs to adsorb CO_2.

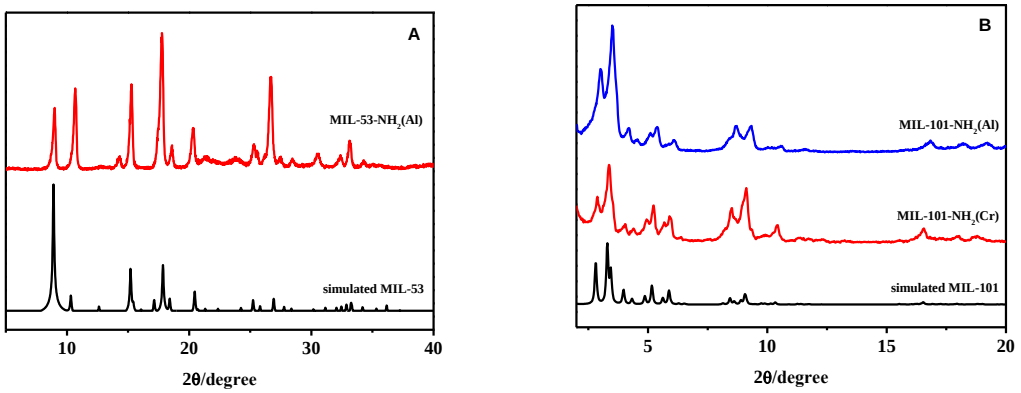

Figure 1. XRD patterns of as-synthesised MIL-53-NH_2(Al) and simulated MIL-53 (A), and as-synthesised MIL-101-NH_2(Al), MIL-101-NH_2(Cr) and simulated MIL-101 (B).

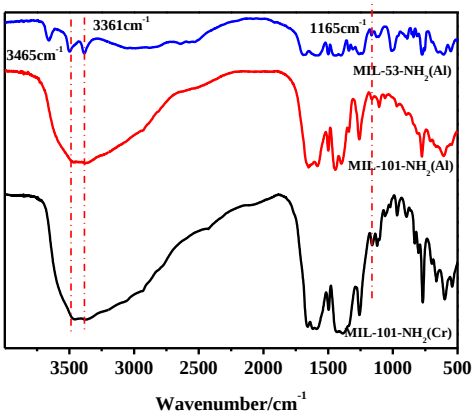

Figure 2. FT-IR spectra of MIL-53-NH_2(Al), MIL-101-NH_2(Al) and MIL-101-NH_2(Cr).

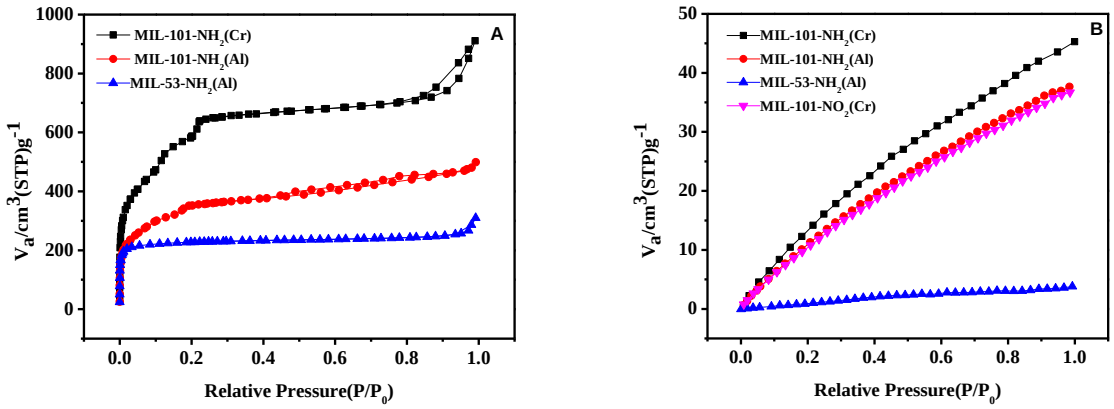

Figure 3. N_2 adsorption−desorption isotherms of MIL-53-NH_2(Al), MIL-101-NH_2(Al) and MIL-101-NH_2(Cr) at 77 K (A) and CO_2 adsorption isotherms of MIL-53-NH_2(Al), MIL-101-NH_2(Al), MIL-101-NH_2(Cr)and MIL-101-NO_2(Cr) at 298 K (B).

Table 1. Textural properties of MIL-53-NH_2(Al), MIL-101-NH_2(Al) and MIL-101-NH_2(Cr).

Samples	BET surface area[a] (m^2 g^{-1})	Average pore size[a] (nm)	Total pore volume[a] (cm^3 g^{-1})	CO_2 adsorbed[b] (cm^3 g^{-1})
MIL-53-NH_2(Al)	849	2.23	0.47	3.80
MIL-101-NH_2(Al)	1250	2.45	0.77	37.63
MIL-101-NH_2(Cr)	1940	3.26	1.41	45.28

[a] Data from N_2 adsorption-desorption isotherms at 77 K. [b] Data from CO_2 adsorption isotherms at 298 K.

Then, CVs of t-Bu(R,R)salen(Co[II]) and PhCH(CH_3)Cl in DMF were studied on MIL-53-NH_2(Al), MIL-101-NH_2(Al), MIL-101-NH_2(Cr) (Fig 4). In the case of MIL-101-NH_2(Cr) (Fig. 4C), when PhCH(CH_3)Cl was dissolved in the electrolyte solution (Fig. 4C, curve b), a reduction peak was found at around -1.74 V. This peak is related to the electroreduction of PhCH(CH_3)Cl to [PhCH(CH_3)]$^-$ (Eq. 1) [38]. After CO_2 introduction (Fig. 4C, curve c), the peak current increased significantly, which indicated that [PhCH(CH_3)]$^-$ could react quickly with CO_2 (Eq. 2). Curve a (Fig. 4C) showed a pair of reversible redox peaks at -1.06 V, which corresponds to the reduction of t-Bu(R,R)salen(Co[II]) to [t-Bu(R,R)salen(Co[I])]$^-$ (Eq. 3) [11,39]. The reduction peak current increased to approximately twice the original when PhCH(CH_3)Cl was added. Moreover, the corresponding oxidation peak disappeared completely (Fig. 4C, curve d). This change corresponded to the organic complex t-Bu(R,R)salen(Co[III])PhCH(CH_3) from the reaction of [t-Bu(R,R)salen(Co[I])]$^-$ and PhCH(CH_3)Cl (Eq. 4) that gained another electron at this potential to obtain the chiral induction intermediate [t-Bu(R,R)salen(Co[II])PhCH(CH_3)]$^-$ (Eq. 5). The big reduction peak at -1.75 V was similar to that in curve b. On the basis of the condition of curve d, CO_2 was bubbled into the solution (Fig. 4C, curve e). Notably, the peak current at -1.10 V increased, which indicated that the chiral induction intermediate reacted with CO_2 (Eq. 6) [11]. Therefore, to obtain optically active products, control of the potential was necessary before the direct electroreduction of PhCH(CH_3)Cl. Similar electrochemical behaviour could be obtained for MIL-53-NH_2(Al) (Fig. 4A) and MIL-101-NH_2(Al) (Fig. 4B). Notably, the corresponding peak

potentials on these materials slightly differed. The reduction peaks of $PhCH(CH_3)Cl$ appeared at -1.69 and -1.63 V on MIL-101-NH_2(Al) and MIL-53-NH_2(Al), respectively. Meanwhile, the potentials of reversible redox peaks that corresponded to Co(II) to Co(I) appeared at -1.07 and -1.08 V, respectively, on MIL-101-NH_2(Al) and MIL-53-NH_2(Al). For comparison, the cyclic voltammograms of solutions that contained $PhCH(CH_3)Cl$, t-Bu(R,R)salen(Co[II]) and CO_2 on three MOFs were summarised in Fig. 4D. Notably, the first reduction peak current on MIL-101-NH_2(Cr) was the largest among these three MOFs. This observation was noted possibly because MIL-101-NH_2(Cr) had the largest specific surface area which provided the most active sites for the combination of substrate and chiral inducer. When MOFs catalyze macromolecular reactions, they must have enough space to allow products and substrates to enter and exit smoothly [40-42]. Large pore size of MIL-101-NH_2(Cr) provides sufficient space for the intermediate [t-Bu(R,R)salen(Co[II])$PhCH(CH_3)$]$^-$ formed by substrate and chiral inducer to react with CO_2 adsorbed in the MOFs. The peak current on MIL-101-NH_2(Al) and MIL-53-NH_2(Al) at this potential were not as large as that of MIL-101-NH_2(Cr), because the specific surface area and pore size of these two MOFs were smaller than MIL-101-NH_2(Cr). The smaller specific surface area provided less active sites; and the smaller pore size made it difficult for larger chiral intermediates to react with the adsorbed CO_2.

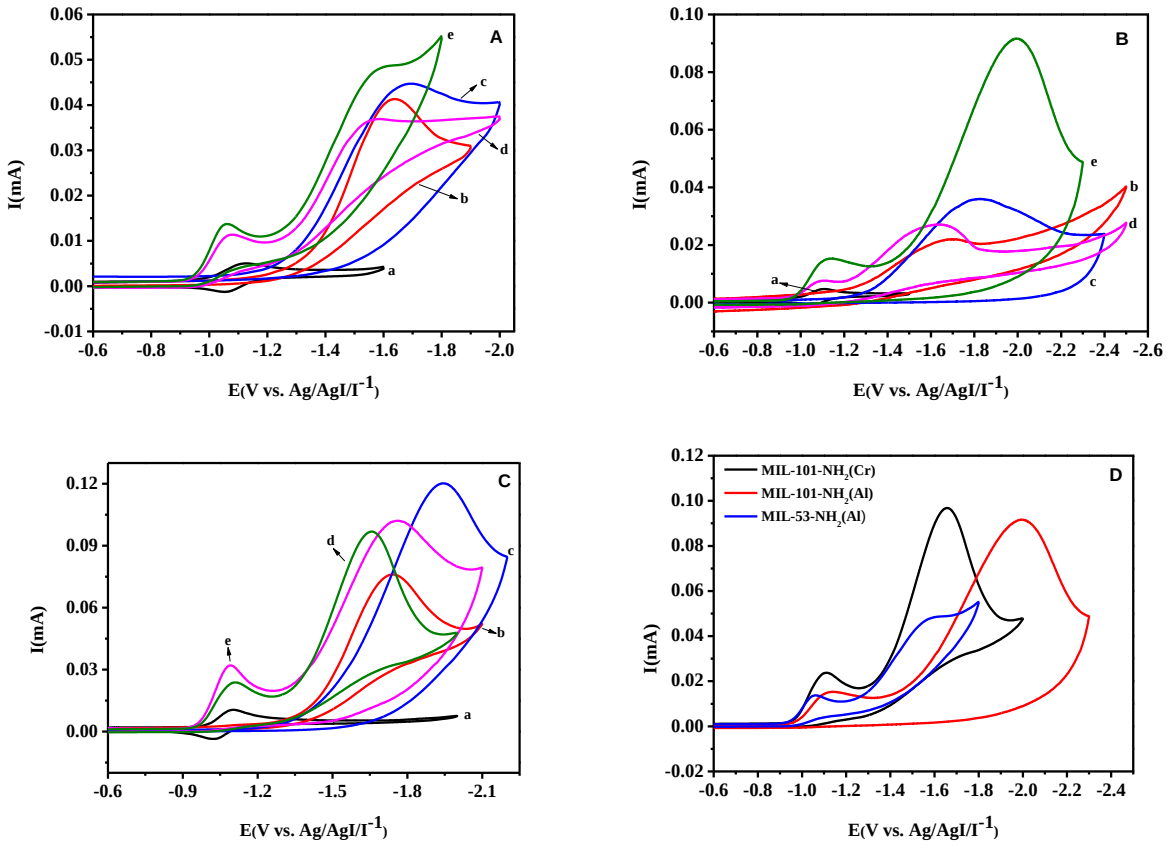

Figure 4. CVs of t-Bu(R,R)salen(Co[II]) and $PhCH(CH_3)Cl$ in DMF-0.1M $TEABF_4$ at MIL-53-NH_2(Al) (A), MIL-101-NH_2(Al) (B) and MIL-101-NH_2(Cr) (C) coated on GC electrode at a scan rate of 0.05 V s^{-1}. (a) 2 mM t-Bu(R,R)salen(Co[II]), (b) 19 mM $PhCH(CH_3)Cl$, (c) as (b) in the presence of 0.2 M CO_2, (d) as (a) + 19 mM $PhCH(CH_3)Cl$, (e) as (d) in the presence of 0.2 M CO_2. (D) CVs at MIL-53-NH_2(Al), MIL-101-NH_2(Al) and MIL-101-NH_2(Cr) coated on GC electrodes in DMF-0.1 M $TEABF_4$-2 mM t-Bu(R,R)salen(Co[II])-19 mM $PhCH(CH_3)Cl$ in the presence of 0.2 M CO_2.

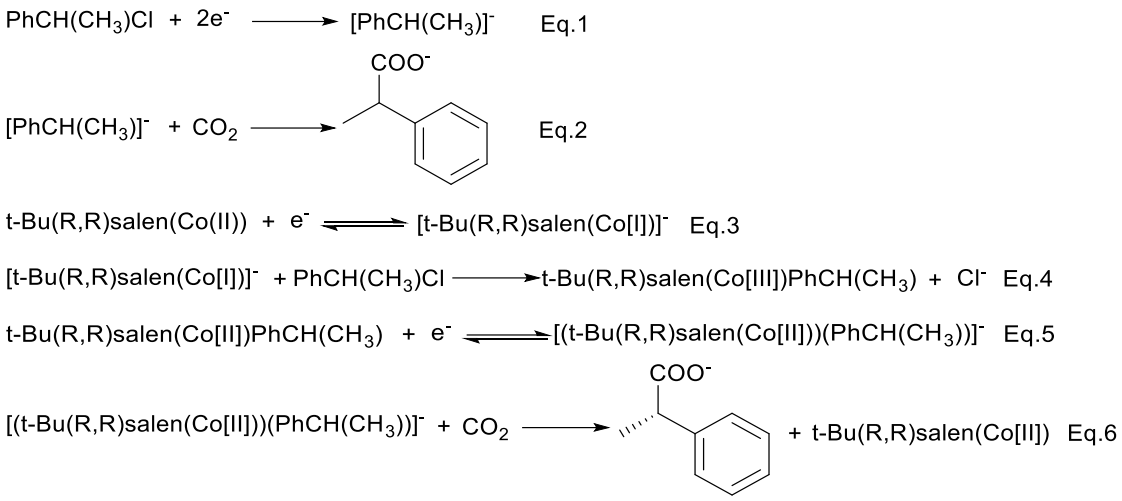

The potentiostatic electrolysis of $PhCH(CH_3)Cl$ with t-Bu(R,R)salen(Co[II]) in the presence of CO_2 was conducted in an undivided cell on MIL-53-NH_2(Al), MIL-101-NH_2(Al) and MIL-101-NH_2(Cr). In the process of potentiostatic electrolysis, the choice of electrolytic potential was very important, especially for this asymmetric electrocarboxylation system. Here, we investigated the effect of electrolytic potential on the reaction from -1.20 V to -1.30 V (Table 2). Taking MIL-53-NH_2(Al) as an example, as the potential shifts negatively, the yield gradually increases, the ee value first increases and then decreases. The other two MOFs also comply with this rule. As described above, $PhCH(CH_3)Cl$ can be carboxylated after its own electroreduction to obtain target carboxylic acid (Eqs. 1 and 2). In addition, carboxylic acid could also be synthesised at more positive potential via electrocatalysis of chiral t-Bu(R,R)salen(Co[II]) (Eq. 3 to Eq. 6). Therefore, the potentials that are controlled around the reduction potential of t-Bu(R,R)salen(Co[II]) and t-Bu(R,R)salen(Co[III])$PhCH(CH_3)$ help increase enantioselectivity. In contrast, the $PhCH(CH_3)Cl$ electrocarboxylation at a more negative potential is not conducive to chiral product formation. In other words, a moderate potential is more conductive to chiral product synthesis.

Then, the effect of the cathode material was investigated. As shown in Table 2 entry 8, when carbon paper was used directly as cathode, the yield was only 3%, and the product was racemic. When MOFs were used as the cathode, the yield was higher and the ee value was moderate. This indicates that MOFs as porous materials play a very important role in the asymmetric electrocarboxylation of $PhCH(CH_3)Cl$. Moreover, at the same potential, the yield and ee value were the best when MIL-101-NH_2(Cr) was used. For MIL-101-NH_2(Cr), which has largest pore size and volume, it may be easy for the intermediate to get in the MOFs and the products to get out from the MOFs, so its corresponding catalytic result is the best. This result is consistent with the cyclic voltammograms (Fig. 4D).

The electrocatalytic performance that was affected by amino groups was also investigated. When MIL-101-NO_2(Cr) was used (Table 2, entry 4), the yield and ee value were 10% and 17%, respectively, which were both significantly lower than those data on MIL-101-NH_2(Cr) (Table 1, entry 7). This finding may be attributed to the different CO_2 adsorption capabilities of these materials. Compared with MIL-101-NO_2(Cr), MIL-101-NH_2(Cr) has a larger amount of CO_2 adsorption (Fig. 3B). Therefore, it might provide more CO_2 during the reaction process, which benefits electrocarboxylation.

Table 2. Influence of cathode materials and potentials on the asymmetric carboxylation of $PhCH(CH_3)Cl$ with CO_2[a]

Entry	E (V vs. Ag/AgI/I^-)	Material	Yield[b] (%)	R-ee[b] (%)
1	-1.20	MIL-53-NH_2(Al)	2	24
2	-1.20	MIL-101-NH_2(Al)	12	16
3	-1.20	MIL-101-NH_2(Cr)	13	21
4	-1.25	MIL-101-NO_2(Cr)	10	17
5	-1.25	MIL-53-NH_2(Al)	5	36
6	-1.25	MIL-101-NH_2(Al)	15	21
7	-1.25	MIL-101-NH_2(Cr)	18	41
8	-1.25	-[c]	3	-[d]
9	-1.30	MIL-53-NH_2(Al)	6	10
10	-1.30	MIL-101-NH_2(Al)	10	9
11	-1.30	MIL-101-NH_2(Cr)	17	37

[a] Solvent: DMF; anode: Pt; substrate: 0.05 M $PhCH(CH_3)Cl$; supporting electrolyte: 0.1 M TEAI; inducer: 7.5 mM t-Bu(R,R)salen(Co[II]); $P_{CO2}=1 \times 10^5$ Pa; temperature: 293 K; Charge: 2 F mol^{-1}. [b] The yield based on the quantity of the starting substrate and ee were measured by HPLC with a chiral AD-H column. [c] Carbon paper without loading MOFs was used. [d] Only racemic product was obtained.

The influence of the electrolysis conditions, such as the amount of catalysts, temperatures and charges, was studied using MIL-101-NH_2(Cr) for the working electrode to optimize the result of asymmetric electrocarboxylation of $PhCH(CH_3)Cl$. Firstly, the effect of catalyst amount was investigated (Table 3, entries 1-4). With increasing catalyst loading amount, the yield and ee value first increased and then decreased. In addition, the highest value was obtained at 20 mg. An increase in the amount of catalysts within a certain range is equivalent to an increase in the active sites, and can increase the amount of CO_2 adsorbed on the electrode surface. These characteristics are conducive to the target electrocarboxylation reaction. However, excessive loading may cause material to pile up and cover the active site, which is not conducive to the mass transfer of substrates and products. The literature [43] also shows that excessive loading is actually not good for catalytic processes. Therefore, in the later part of the loading increases, the catalytic performance declined. Secondly, the temperature effect on the reaction was investigated. As shown in Table 3 (entries 3, and 5-8), 293 K was the most optimal temperature. High reaction temperature can speed up the reaction rate but reduce CO_2 solubility. Therefore, a moderate reaction temperature is conductive to the asymmetric electrocarboxylation. Finally, the effect of charge on the reaction was determined (Table 3, entries 9-11). Addition of charge will increase the number of electron transfers. Thus, more [t-Bu(R,R)salen(Co[II])$PhCH(CH_3)$]$^-$ will react with CO_2. As the charge increased, the yield and ee also increased. After a certain degree, the yield did not change, but the ee value decreased significantly. Therefore, the optimal charge is 3 F mol^{-1}.

As it is difficult to electrochemically fix CO_2 stereoselectively, there are few reports on the same reaction about asymmetric electrocarboxylation of organic compounds in CO_2 atmosphere. Compared with our previous report on asymmetric electrocarboxylation of (1-chloroethyl)benzene with CO_2 [11], although the ee value in this work is not satisfactory, the electrolytic conditions are relatively mild, and the reaction can be performed at room temperature.

Table 3. Influence of cathode materials and potentials on the asymmetric carboxylation of $PhCH(CH_3)Cl$ with CO_2[a]

Entry	Amount of Catalysts (mg)	T (K)	Charge ($F \cdot mol^{-1}$)	Yield[b] (%)	R-ee[b] (%)
1	10	293	2	11	17
2	15	293	2	16	44
3	20	293	2	18	41
4	25	293	2	19	30
5	20	283	2	13	17
6	20	303	2	12	33
7	20	313	2	10	26
8	20	323	2	10	13
9	20	293	1	14	28
10	20	293	3	29	51
11	20	293	4	26	35

[a] Solvent: DMF; cathode: MIL-101-NH_2(Cr); anode: Pt; substrate: 0.05 M $PhCH(CH_3)Cl$; supporting electrolyte: 0.1 M TEAI; inducer: 7.5 mM t-Bu(R,R)salen(Co[II]); $P_{CO2}=1 \times 10^5$ Pa; [b] The yield based on the quantity of the starting substrate and ee were measured by HPLC with a chiral AD-H column.

4. CONCLUSIONS

Considering that the amino-functionalized MOFs of MIL types have good stability and CO_2 adsorption capacity, we firstly used MIL-101-NH_2(Cr), MIL-101-NH_2(Al), MIL-53-NH_2(Al) as heterogeneous catalysts for the asymmetric electrocarboxylation of (1-chloroethyl)benzene. MIL-101-NH_2(Cr) had the largest specific surface area and pore size and was modified with amino groups. Therefore, this compound exhibited good affinity for CO_2. Using t-Bu(R,R)salen(Co[II]) as chiral intermediate, MIL-101-NH_2(Cr) showed good catalytic effect in asymmetric electrocarboxylation of (1-chloroethyl)benzene to obtain optically active 2-phenylpropionic acid under mild synthesis conditions.

ACKNOWLEDGEMENTS
Financial support from National Natural Science Foundation of China (21673078 and 21773071) is gratefully acknowledged.

References

1. R. Quadrelli and S. Peterson, *Energy Policy*., 35(2007)5938.
2. J. Qiao, Y. Liu, F. Hong and J. Zhang, *Chem Soc Rev*., 43(2014)631.
3. M. North, R. Pasquale and C. Young, *Green Chem*., 12(2010)1514.
4. L. X. Wu, Y. G. Zhao, Y. B. Guan, H. Wang, Y. C. Lan, H. Wang and J. X. Lu, *RSC Adv*., 9(2019)32628.
5. K. Zhang, Y. Xiao, Y. Lan, M. Zhu, H. Wang and J. Lu, *Electrochem. Commun*., 12(2010)1698.

6. H. M. Wang, G.-J. Sui, D. Wu, Q. Feng, H. Wang and J.-X. Lu, *Tetrahedron*., 72(2016)968.
7. R. Matthessen, J. Fransaer, K. Binnemans and D.E.D. Vos, *RSC Adv*., 3(2013)4634.
8. S. F. Zhao, M. Horne, A. M. Bond and J. Zhang, *Green Chem.*, 16(2014)2242.
9. B. L. Chen, Z. Y. Tu, H. W. Zhu, W. W. Sun, H. Wang and J. X. Lu, *Electrochim. Acta*., 116(2014)475.
10. H. P. Yang, Y. N. Yue, Q. L. Sun, Q. Feng, H. Wang and J. X. Lu, *Chem. Commun.*, 51(2015)12216.
11. B. L. Chen, H. W. Zhu, Y. Xiao, Q. L. Sun, H. Wang and J. X. Lu, *Electrochem. Commun*., 42(2014)55.
12. Y. C. Lan, H. Wang, L. X. Wu, S. F. Zhao, Y. Q. Gu and J. X. Lu, *J. Electroanal. Chem*., 664(2012)33.
13. H. Wang, X. M. Xu, Y. C. Lan, H. M. Wang and J. X. Lu, *Tetrahedron*., 70(2014)1140.
14. J. R. Li, R. J. Kuppler and H. C. Zhou, *Chem. Soc. Rev*., 38(2009)1477.
15. L. J. Murray, M. Dinca and J. R. Long, *Chem. Soc. Rev*., 38(2009)1294.
16. B. D.Chandler, D. T. Cramb and G. K. H. Shimizu, *J. Am. Chem. Soc*., 128(2006)10403.
17. Y. K. Hwang, D. Y. Hong, J. S. Chang, S. H. Jhung, Y. K. Seo, J. Kim, A. Vimont, M. Daturi, C. Serre and G. Ferey, *Angew. Chem. Int. Ed. Engl*., 47(2008)4144.
18. H. Yang and J. R. Li, *Porous Materials for Carbon Dioxide Capture*, Springer,(2014) Berlin,Germany.
19. R. Senthil Kumar, S. Senthil Kumar and M. Anbu Kulandainathan, *Electrochem. Commun*., 25(2012)70.
20. Y. Zhang, X. Bo, A. Nsabimana, C. Han, M. Li and L. Guo, *J. Mater. Chem. A*., 3(2015)732.
21. J. Wang, M. Yang, W. Dong, Z. Jin, J. Tang, S. Fan, Y. Lu and G. Wang, *Catal. Sci. Technol*., 6(2016)161.
22. D. B. Dang, P. Y. Wu,C. He, Z. Xie and C. Y. Duan, *J. Am. Chem. Soc*., 132(2010)14321.
23. G. Fe´rey, C. Serre, F. Millange, J. Dutour, S. Surble´, and I. Margiolaki, *Science*., 309(2005)2040.
24. J. Gascon, U. Aktay, M. Hernandezalonso, G. Vanklink and F. Kapteijn, *J. Catal*., 261(2009)75.
25. J. C. Hicks, J. H. Drese, D. J. Fauth, M. L. Gray, G. Qi and C. W. Jones, *J. Am. Chem. Soc*., 130(2008) 2902.
26. Y. Luo, H. H. Funke, J. L. Falconer and R. D. Noble, *Industrial & Engineering Chem. Res.*, 55(2016)9749.
27. R. E. Morris and P. S. Wheatley, *Angew Chem Int Ed Engl*., 47(2008)4966.
28. J. S. Lee, J. T. Kim, J. K. Suh, J. M. Lee,C. H. Lee, *J. Chem. Eng.Data*., 47(2002)1237.
29. R. Babu, A. C. Kathalikkattil, R. Roshan, J. Tharun, D. W. Kim and D. W. Park, *Green Chem*., 18(2006)232.
30. T. Lescouet, C. Chizallet and D. Farrusseng, *ChemCatChem*., 4(2012)1725.
31. S. Bernt, V. Guillerm, C. Serre and N. Stock, *Chem. Commun (Camb).*, 47(2011)2838.
32. X. Cheng, A. Zhang, K. Hou, M. Liu, Y. Wang, C. Song, G. Zhang and X. Guo, *Dalton Trans*., 42(2013)13698.
33. M. Hartmann and M. Fischer, *Micro. Meso. Mater*., 164(2012)38.
34. Y. Lin, C. Kong and L. Chen, *RSC Adv*., 2(2012)6417.
35. P. Serra-Crespo, E. V. Ramos-Fernandez, J. Gascon and F. Kapteijn, *Chem. Mater*., 23(2011)2565.
36. J. Gascon, U. Aktay, M. Hernandezalonso, G. Vanklink and F. Kapteijn, *J. Catal*., 261(2009)75.
37. B. Arstad, H. Fjellvåg, K. O. Kongshaug, O. Swang and R. Blom, *Adsorption*., 14(2008)755.
38. A. A. Isse, M. G. Ferlin and A. Gennaro, *J. Electroanal. Chem*., 541(2003)93.
39. A. A. Isse, A. Gennaro and E. Vianello, *J. Chem. Soc. Dalton*, (1996)1613.
40. C. Zhu, Q. Xia, X. Chen, Y. Liu, X. Du and Y. Cui, *ACS Catal*., 6(2016)7590.
41. L. Ma, J. M. Falkowski, C. Abney and W. Lin, *Nat. Chem*. 2(2010)838.
42. C. W. Feijie Song, Joseph M. Falkowski, Liqing Ma, and Wenbin Lin, *J. Am. Chem. Soc*., 132(2010)15390.

43. E. Niknam, F. Panahi, F. Daneshgar, F. Bahrami and A. Khalafi-Nezhad, *ACS Omega*., 3(2018)17135.